In Silico Analysis, Biological Activity, and ADME Profiling of Flavonoid Compounds Targeting RNA-Dependent RNA Polymerase of DENV-3

Siti Zainatun Wasilah[1,2], Tri Wibawa[3*], and Nastiti Wijayanti[4]

[1]*Doctoral Program in Medical and Health Sciences, Faculty of Medicine, Public Health and Nursing, Universitas Gadjah Mada, Sekip Utara, Yogyakarta 55281, Indonesia*

[2]*Medical Laboratory Technology, Poltekkes Kemenkes Yogyakarta, Jl. Ngadinegaran MJ III/62, Yogyakarta 55141, Indonesia*

[3]*Department of Microbiology, Faculty of Medicine, Public Health and Nursing, Universitas Gadjah Mada Sekip Utara, Yogyakarta 55281, Indonesia*

[4]*Laboratory of Animal Physiology, Faculty of Biology, Universitas Gadjah Mada, Jl. Teknika Selatan, Sekip Utara, Yogyakarta 55281, Indonesia*

* ***Corresponding author:***

email: twibawa@ugm.ac.id

Received: July 7, 2025
Accepted: September 1, 2025

DOI: 10.22146/ijc.108797

Abstract: *Dengue virus (DENV) remains a global health challenge. DENV-3 is the most virulent of the four dengue virus serotypes, requiring the identification of new inhibitors against RNA-dependent RNA polymerase (RdRp), an essential enzyme for viral replication. This study evaluated the inhibitory potential of flavonoids, including quercetin, fisetin, myricetin, daidzein, and ribavirin. Molecular docking revealed binding energies of −8.0, −7.4, −7.3, and −7.4 kcal/mol for quercetin, fisetin, myricetin, and daidzein, respectively, exceeding those of ribavirin as a control (−5.6 kcal/mol). These ligands exhibit strong interactions with active site residues, including hydrogen bonds and hydrophobic interactions. Molecular dynamics simulations of 100 ns confirmed a stable protein-ligand complex, with quercetin showing a stable RMSD and RoG values compared to the control, indicating good binding stability. SASA and hydrogen bond analysis support the stability of quercetin interactions. Pharmacokinetic evaluation shows that four ligands comply with Lipinski's rules of five, supporting their potential as drug candidates. These findings highlight the potential of quercetin, fisetin, myricetin, and daidzein as DENV-3 RdRp inhibitors, with quercetin as the most effective, with the lowest binding energy and inhibition constant. Experimental validation is needed to explore the potential antiviral effects of DENV.*

Keywords: *flavonoids; DENV-3; molecular docking; molecular dynamics; quercetin*

■ INTRODUCTION

Dengue infection is a disease transmitted through the bite of *Aedes* mosquitoes, including those of *Aedes aegypti* and *Aedes albopictus*. Globally, this mosquito-borne disease is considered the most common arbovirus infection in humans [1]. Dengue virus (DENV) is part of the *Flaviviridae* family, which contains more than 70 major human pathogens. Most of these pathogens affect the tropics, with around 3.9 billion people infected [2]. DENV is responsible for causing diseases that are potentially life-threatening and pose a significant public health risk worldwide. Dengue infection is caused by four antigenically and genetically distinct serotypes, including DENV 1-4 [3].

The spectrum of DENV infection can vary from undifferentiated febrile illness or asymptomatic infection to more serious manifestations, including dengue shock syndrome (DSS) and dengue hemorrhagic fever (DHF). DSS is considered the most severe form of clinical syndrome and involves plasma leakage, blood clotting irregularities, and increased vascular fragility. In addition, an increased level of capillary permeability can lead to multiple organ failure and hypovolemic shock.

The transmission and incidence of DHF are influenced by various factors, such as lack of effective vector control, poor waste management systems, urbanization, and uncontrolled population growth [4]. Several other factors, including the epidemiological context, host immunity, genetics, and viral characteristics, can also make significant contributions in providing protection or increasing the DHF incidence. In addition, the dengue vaccine, which is considered a major public health effort against infectious disease, has not yet shown a significant impact on dengue infection control [5].

DENV is a positive-strand RNA virus containing an 11kb genome and a large open reading frame (ORF), which is translated into one complete polyprotein that is then processed into various other proteins. The RNA genome encodes a polyprotein that undergoes proteolytic cleavage to produce three structural proteins, capsid (C), precursor membrane (prM) or membrane (M), an envelope protein (E), and seven non-structural proteins (NS1, NS2A, NS2B, NS3, NS4A, NS4B, and NS5). The E and prM/M proteins are located on the surface of DENV virions. In contrast, the C protein encapsulating the RNA genome is situated under the lipid layer of structural proteins that comprise the viral particle. Non-structural proteins are essential components of the DENV life cycle for viral replication, assembly, maturation, and polyprotein division [6].

Despite the significant economic and social impacts of the DENV infection and the important progress made against Dengue, no effective antiviral therapies are currently available. Considering these limitations, research should be done to find molecules, compounds, or drugs that can inhibit enzymatic targets or processes critical to the viral replication cycle. The development and search for therapeutic molecules, such as direct-acting antivirals (DAAs), have proven to be an effective approach [7-8]. Compounds that can inhibit the replication of DENV have the potential to be developed as DENV antivirals. Non-structural protein 3 (NS3), a protein found inside cells, consists of two domains, namely protease and helicase. Proteases play a role in cutting polyproteins that are important for viral replication in the cell, while helicases function in the replication process of viral genetic material. Non-structural protein 5 (NS5) also consists of two domains, namely methyltransferase and RNA-dependent RNA polymerase (RdRp), both of which play a role in viral RNA replication. The RdRp domain is essential for the synthesis of both positive- and negative-strand RNA during replication. Since no similar protein exists in humans, RdRp is a potential target for the development of DENV-specific antiviral inhibitors [9]. This means that inhibitors targeting the RdRp enzyme can be designed to selectively target the virus without causing significant side effects on human cells, making RdRp inhibitors safer compared to drugs targeting cellular proteins with homologs in the human body. Given its crucial role, DENV-3 RdRp is an attractive target for antiviral drug development, as inhibiting its activity can effectively halt viral replication [10].

The use of computational techniques that have been used in other studies was considered an attractive strategy. The flavonoids, fisetin and quercetin, against spike proteins using *in silico* docking simulations, both have a binding affinity value of −8.5 kcal/mol against the S2 domain of the SARS-CoV-2 spike protein [11]. The flavonoid myricitrin has a high binding affinity with a binding energy score of −8.9 kcal/mol against the main protease enzyme of SARS-CoV-2 via molecular docking [12]. Quercetin has also shown inhibitory activity against SARS-CoV-2. All of this demonstrates the potential of flavonoids as antiviral properties [13-14]. Database screening and docking analysis are promising for selecting targets of action, such as essential proteins in the viral infection cycle, with the viral NS5 polymerase protein prominent among them. Flavonoids are a category of low-molecular polyphenolic compounds produced exclusively in plants. Flavonoids have various biological and pharmacological functions, namely anti-allergic, anti-inflammatory, antioxidant, antibacterial, antifungal, antiviral, anticancer, and antidiarrheal [15-18]. Quercetin is a natural flavonoid that has been proven to have anti-hepatitis C virus (HCV) properties, influenza [19-20], DENV-2, and pseudorabies [21-22]. Fisetin has been shown to be an effective antiviral agent against CHIKV by modulating apoptosis and oxidative

stress pathways [23], antiviral activity against fish pathogenic infectious hematopoietic necrosis virus (IHNV) and viral hemorrhagic septicemia virus (VHSV) [24]. Myricetin demonstrates antiviral effects against both Chikungunya virus (CHIKV) and pseudorabies virus, highlighting its potential as a therapeutic candidate [25-27]. Daidzein inhibits influenza virus replication via signal transduction through 5-lipoxygenase products and antiviral DENV-2 [21,28].

DENV-3 is a dengue virus serotype that often triggers outbreaks [28], especially in tropical and subtropical regions. Infection caused by DENV-3 can lead to a significant increase in the number of dengue fever cases. In dengue fever, the severity of the disease is directly related to the viral load [29]. Therefore, the RNA-dependent RNA polymerase enzyme, which plays a crucial role in viral replication, has been selected as a therapeutic target. Antiviral research on DENV-3 using quercetin, fisetin, myricetin, and daidzein is still limited, necessitating further investigation. We conducted computational screening of these four compounds against the DENV-3 polymerase enzyme and followed up with molecular dynamics (MD) simulations to verify the results. This study successfully identified key residues and interactions that influence the activity and potential of the proposed compounds.

In silico approaches, including molecular docking, MD simulations, and absorption, distribution, metabolism, and elimination (ADME) prediction, have played an important role in the discovery of DENV-3 RdRp inhibitors. These computational methods enable rapid screening of large libraries of flavonoids, identification of potential binding interactions, and optimization of alternative molecules prior to experimental validation. Such approaches have significantly accelerated the drug discovery process, reducing time and costs while improving the accuracy of selecting promising candidates for further *in vitro* and *in vivo* studies [30]. The study aims to provide deeper insights into the DENV-3 RdRp protein and its interactions with several flavonoids that have potential as antiviral agents, namely quercetin, fisetin, myricetin, and daidzein. This study compared these compounds with ribavirin as a control in terms of biological activity, ADME, as well as PASS prediction, molecular docking, and MD simulations.

■ EXPERIMENTAL SECTION

Materials and Instrumentation

The materials used in this study included the structures of four flavonoids: quercetin, fisetin, myricetin, and daidzein, along with ribavirin as a control, all of which were used for molecular docking against the DENV-3 RdRp protein structure. The structure model of DENV-3 RdRp complexed with the natural ligand 5-{[(4-chlorophenyl)sulfonyl]amino}-2-methyl-1-benzofuran-3-carboxylic acid (PDB ID: 3VWS) is shown in Fig. 1. The structures of the proposed compounds obtained from PubChem are demonstrated in Fig. 2.

The tools used in this study included hardware consisting of a personal computer with an AMD Ryzen 9 5900X processor and an RTX 3050 graphics card. The software used was Autodock Vina [31] to perform molecular docking and AutoDockTools 1.5.6 to set the parameters for molecular docking simulations. PyMOL (https://pymol.org) and Open Babel (https://open-babel.readthedocs/io/en/latest/) were used to calculate the root mean square deviation (RMSD) value of redocking results. BIOVIA Discovery Studio 2021 (https://discover.3ds.com/discovery-studio-visualizer) was utilized to perform ligand and receptor preparation

Fig 1. Structure of DENV-3 RdRp complex

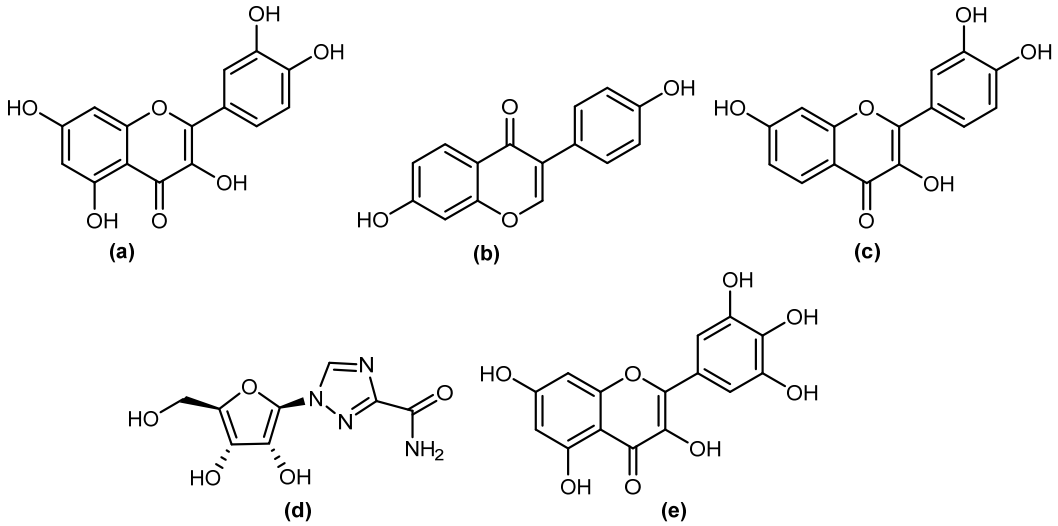

Fig 2. Chemical structure of (a) quercetin, (b) fisetin, (c) myricetin, (d) daidzein, and (e) ribavirin

and visualize non-covalent interactions between ligand and receptor. YASARA structure [32-33] was used for MD simulations. Protein Data Bank (https://www.rscb.org) and PubChem (https://pubchem.ncbi.nlm.nih.gov) were among the websites used in this study.

Procedure

Receptor preparation

The macromolecule DENV-3 RdRp was downloaded from the protein database with PDB ID: 3VWS in PDB format [34]. The downloaded receptor was pretreated using Discovery Studio 2021 to separate the protein from natural ligands and water molecules. DENV-3 RdRp and natural ligands that have been separated were stored in *pdb format. Prepared receptors were then added polar hydrogen and Kollman charges using AutoDock Tools 1.5.6 software and saved in PDBQT format.

Preparation of natural ligand and test ligands

The natural ligand 5-{[(4-chlorophenyl)sulfonyl]amino}-2-methyl-1-benzofuran-3-carboxylic acid (NITD-107) as a comparator and test ligands of four flavonoid compounds: quercetin, fisetin, myricetin, daidzein, and one drug control (ribavirin) were obtained from PubChem in SDF format and then converted to PDB format using Open Babel. Ligands were optimized using AutoDockTools by setting the torsion tree and then saved in pdbqt format.

Redocking process

Ligands and receptors were then optimized in pdbqt format, which began by forming a grid box or a place for molecular docking. The active side of this binding was set with a grid box at coordinates X = 30.89, Y = 61.48, Z = 14.45 Å with a size of 14 × 14 × 14 Å, respectively, with a line spacing of 1 Å. The molecular docking process was first carried out with its natural ligand and should get a RMSD value smaller than 2 Å for molecular docking parameter validity [35]. The redocking process is used to check whether the applied docking protocol can produce accurate predictions. If the RMSD value is less than 2 Å, it means that the model successfully placed the ligand in the correct position, as in the original structure [36]. However, if the RMSD was greater than 2 Å, the model cannot place the ligand accurately, which reduces confidence in the docking results. In addition, a low RMSD value also means that the interaction between the ligand and the protein was stable, which increases the likelihood that the ligand can inhibit protein function more effectively due to its stronger bond at the protein's active site [37]. RMSD value was calculated using PyMOL. If these conditions are met, the molecular docking method for the compound can be proposed.

Molecular docking

A valid docking process was carried out on the test ligand and the comparison ligand against each target protein through AutoDock Vina software, referring to redocking where the values of x, y, and z are 30.89, 61.48, and 14.45, respectively, with a grid box volume of 14 × 14 × 14 Å, respectively, with a line spacing of 1 Å. The docking process ran with the help of a command prompt through the Vina configuration in Notepad format. The vina configuration contains the receptor and ligand names, outputs, and grid boxes that have been adjusted. Results from the docking process were created in pdbqt format. The process run by the command prompt was encoded with the command "--config conf.txt --log log.txt". The docking results were expressed by the binding affinity and amino acid residue interaction values. The docking results were visualized using Discovery Studio Visualizer and PyMOL software and analyzed using AutoDock tools with parameters of binding energy (ΔG), inhibition constant (Ki), and RMSD, as well as visualization results after analyzing ligand and amino acid interactions.

Visualization of docking results

The ligand-receptor complex in pdbqt format was visualized to review the results visually using the Discovery Studio 2021 software to see the ligands' interactions with the receptors in two dimensions. The ligands and receptors showed the presence of hydrogen bond interactions, hydrophobic interactions, and other interactions on the active side of DENV-3 RdRp.

MD simulation

DENV-3 RdRp receptors and ligands prepared from the best MD results were simulated using molecular dynamics simulation in the YASARA structure [32-33] application. The best molecular docking results of modified quercetin, fisetin, myricetin, daidzein, and ribavirin compounds were saved in PDB format and used as material to run MD simulation. MD simulations were run using the default MD macro parameter file of the YASARA structure [32], which has been adjusted to the environmental conditions of each protein. In protein 3VWS, simulations were carried out using the file "md_run.mcr" with pH 7.4 at a temperature of 310 K and a pressure of 1 bar. Each simulation was run with the AMBER14 force field for 100 ns, with snapshots saved every 100 ps. MD simulation results were analyzed using the default "md_analyze.mcr" file from YASARA structure software. After the simulation, visualization analysis was performed using Discovery Studio.

Predicted pharmacokinetics and toxicity aspects

Pharmacokinetic properties using the SwissADME online site (http://www.swissadme.ch/index.php) were predicted by copying the SMILES code from the PubChem database (https://pubchem.ncbi.nlm.nih.gov/). ADME analysis results were compared and adjusted with ADME parameters [38].

Biological activity analysis

The prediction of activity spectra for substances (PASS) (https://www.way2drug.com/passonline/) was employed to predict bioactivity spectra. The PASS analysis provided two probabilities of active molecules (Pa) and a probability of inactivity (Pi). The values of Pa and Pi ranged between 0 and 1. Higher Pa and lower Pi indicate a greater likelihood of the predicted activity being experimentally confirmed. PASS test was analyzed by classifying the Pa (Probable activity) value of the activity test results of flavonoid compounds as antiviral. If the Pa value is more than 0.3 (Pa > 0.3), it was proven low on the silico scale. While if the Pa value is 0.5–0.7 (0.5 < Pa < 0.7), it was proven good *in silico* and medium laboratory scales. If the Pa value was more than 0.7 (Pa > 0.7), it was demonstrated as a high laboratory scale [39-40].

■ RESULTS AND DISCUSSION

Molecular Docking

Parameters observed in the initial docking results were the analysis of ΔG and Ki, which are directly related to the strength of binding affinity. Binding affinity becomes crucial in evaluating the interactions between the ligands and the receptors. The lower the binding affinity value, the less energy the compound requires to interact with its receptor. ΔG analysis aims to evaluate the extent to which a reaction proceeds spontaneously as well as assess the stability of the interactions between ligands and receptors. The lower (negative) the ΔG

value, the more stable the complex formed. The stability of this interaction also indicates the ability of the compound to form a strong chemical bond with the target receptor. Experimentally, ΔG is directly related to Ki, in accordance with the ΔG = −RT In Ki. Thus, the ΔG value can be used to predict a compound's ability to inhibit proteins. The docking results of flavonoid test compounds showed that all test compounds had ΔG < 0, illustrating that the compounds had an affinity to the active side of the DENV-3 RdRp receptor. The five test compounds in this study presented low ΔG and Ki values (Table 1). Among the five test compounds, quercetin exhibited the best affinity, with the lowest ΔG and Ki values of −8.0 kcal/mol and 1.35 μM, respectively.

Fig. 3(a) shows the interaction of native ligands by forming two bonds, namely hydrogen bonds (green) and hydrophobic bonds (purple). Native ligands form hydrogen bonds with Gly604. Hydrophobic bonds form carbon-hydrogen bonds with Val603, van der Waals bonds with Asn405, Gly601, Gln602, Val603, Thr605, Tyr606, Arg792, Trp795, Ser796, and pi-alkyl bonds with Phe412, Trp477, Arg481, and Ile797. Residues Arg792 and Trp795 at the RdRp catalytic site interact directly with the native ligand. Trp795 helps stabilize the ligand through hydrophobic interactions, while Arg792 plays a role in stabilizing the ligand through electrostatic interactions with the RNA phosphate backbone, supporting the catalytic mechanism and RNA replication of the virus. Both residues are crucial for the binding efficiency and catalytic activity of RdRp [41]. The residues on the native ligand compared to the residues on the ribavirin compound (control) are the residues on the hydrogen bond (Gly604), the residues on the van der Waals bonds (Asn405, Phe412, Gly601, Gln602, Val603, Thr605, Tyr606, Arg792, and Trp795). This suggests that the native ligand and the control have similar binding mechanisms, allowing both to interact in a similar manner at the active site. Fig. 3(b) conveys the binding interaction between quercetin and the receptor, which forms two bonds: a hydrogen bond (green) and a hydrophobic bond (purple). Quercetin forms hydrogen bonds with Asn492, Gln602, and Ser798. Quercetin interacts with hydrophobic bonds, including van der Waals bonds with

Table 1. ΔG and Ki results

Test compound	PubChem ID	ΔG (kcal/mol)	Ki (μM)
Native ligand	-	−7.7	2.25
Quercetin	5280343	−8.0	1.35
Fisetin	5281614	−7.4	3.73
Myricetin	5281672	−7.3	4.42
Daidzein	5281708	−7.4	3.70
Ribavirin	37542	−5.6	7.80

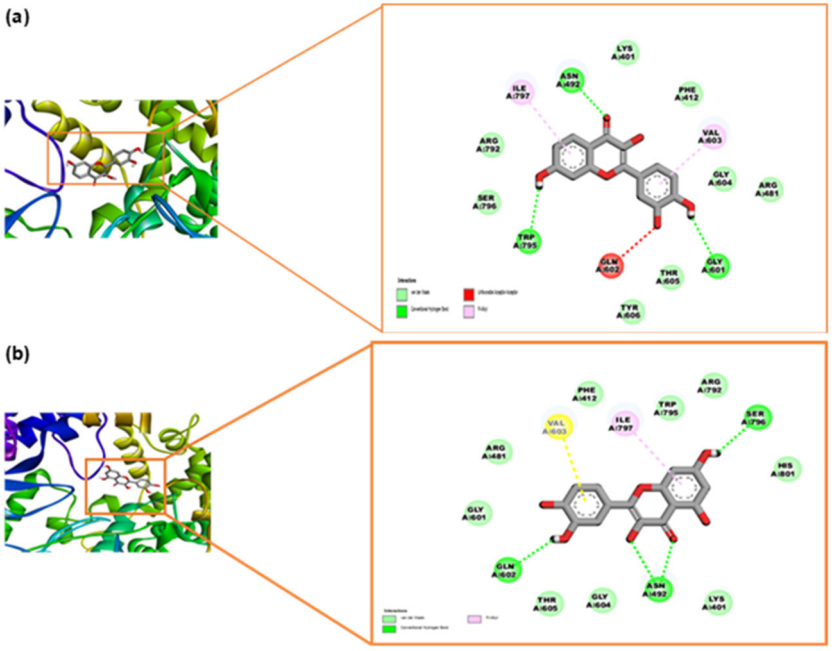

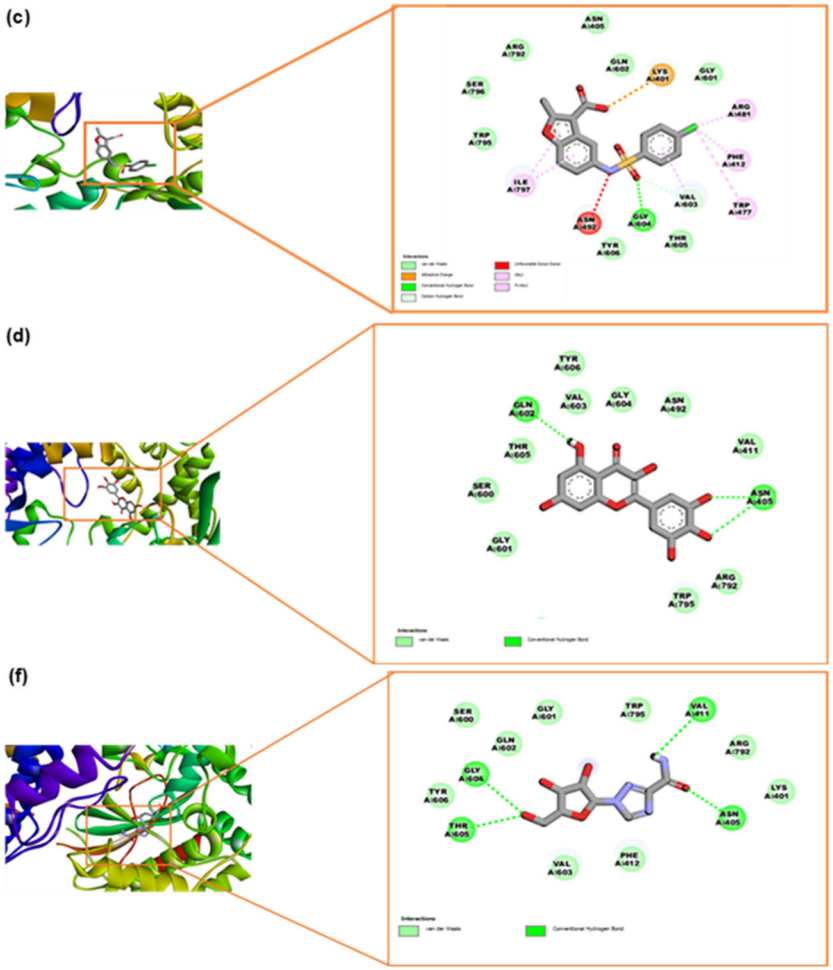

Fig 3. Molecular docking configuration and interaction with target proteins. The complex protein-ligand interactions of (a) native ligand, (b) quercetin, (c) fisetin, (d) myricetin, (e) daidzein, and (f) ribavirin (control)

Lys401, Phe412, Arg481, Gly601, Gly604, Thr605, Arg792, Trp795, and His801, and pi-alkyl bonds with Val603 and Ile797. Quercetin interacts with active residues in the catalytic site of the protein through various types of bonds that enhance the stability and effectiveness of ligand binding. Trp795 plays an important role in hydrophobic interactions, which maintain the precise position of the ligand, while Arg792 interacts electrostatically with quercetin, stabilizing the complex and supporting the catalytic mechanism. Phe412 contributes through hydrophobic bonds, strengthening quercetin's stability in the active site, and Val603 interacts through Pi-Alkyl bonds, contributing to the strength of the bond between the ligand and the protein. This combination of interactions demonstrates that quercetin has strong and effective binding potential, which can enhance its biological activity in inhibiting the target protein [41-42]. The residues on quercetin compared to the residues on the ribavirin compound (control) are the residues on the hydrogen bond (Gly604), the residues on the van der Waals bond (Lys401, Phe412, Gly601, Val603, Arg792, and Trp795). This may indicate that quercetin and the control have similar binding mechanisms, allowing both to interact in a similar manner at the active site.

Fig. 3(c) reveals that the binding interaction between the fisetin compound and the receptor forms hydrogen bonds (green) and hydrophobic bonds (purple). The fisetin compound forms hydrogen bonds with Asn492, Gly601, Trp795, hydrophobic bonds,

including van der Waals bonds with Lys401, Phe412, Arg481, Gly604, Thr605, Tyr606, Arg792, and Ser796, and pi-alkyl bonds with Val603 and Ile797. The interaction between fisetin and the receptor involves various non-covalent bonding forces that enhance the stability of the protein-ligand complex. Arg792 interacts electrostatically with fisetin, strengthening its bond, while Trp795 is involved in pi-stacking, which maintains the position of fisetin in the active site. Phe412 interacts through hydrophobic bonds, strengthening the binding with aromatic residues, and Val603 contributes to stability with Pi-Alkyl. These interactions indicate that fisetin binds strongly to the receptor, enhancing its potential as a therapeutic compound. The residues on fisetin compared to the residues on the ribavirin compound (control) are the residues on the hydrogen bond (Gly604), the residues on the van der Waals bond (Phe412, Gly601, Val603, Arg792, and Trp795). This may indicate that fisetin and the control have similar binding mechanisms, allowing both to interact in a similar manner at the active site.

Fig. 3(d) shows the interaction between myricetin and the receptor, which forms a single bond, namely a hydrogen bond (green). Myricetin forms hydrogen bonds with Asn405 and Gln602. Hydrophobic bonds, including van der Waals bonds, are formed with Val411, Asn492, Ser600, Gly601, Val603, Gly604, Thr605, Tyr606, Arg792, and Trp795. Myricetin interacts with the protein's active site through a combination of hydrogen bonds and hydrophobic bonds, which increase the stability and strength of ligand binding. Hydrogen bonds are formed with Asn405 and Gln602, which help stabilize the position of myricetin in the active site with more specific and targeted interactions. Additionally, hydrophobic bonds, including van der Waals forces, form with various residues such as Val603, Gly604, Tyr606, and Trp795, contributing to the strengthening of non-covalent interactions between myricetin and the target protein. These hydrophobic bonds are crucial for maintaining the ligand's position and ensuring its effectiveness in inhibiting protein activity. The residues on myricetin compared to the residues on the ribavirin compound (control) are the residues on the hydrogen bond (Asn405), the residues on the van der Waals bond (Phe412, Val603, Arg792, and Trp795). This may indicate that myricetin and the control have similar binding mechanisms.

Fig. 3(e) shows that the binding interaction between daidzein and the receptor does not form hydrogen bonds but instead forms hydrophobic bonds, specifically carbon-hydrogen bonds with Val411. Van der Waals interactions with Phe398, Lys401, Thr413, and Phe485. Pi-pi interactions with Val411. Pi-pi stacked interactions with Phe412 and Trp795. Pi-pi shaped interactions with Phe412 and Trp795. The interaction between daidzein and the receptor shows that even though there are no hydrogen bonds, daidzein forms strong non-covalent interactions. Hydrophobic bonds occur with Val411, while van der Waals interactions are formed with residues Phe398, Lys401, Thr413, and Phe485, which strengthen ligand binding in the active site. Pi-pi and pi-pi stacked interactions with Phe412 and Trp795 also contribute to the stability of daidzein's position in the active site. These interactions indicate that daidzein binds strongly to the receptor through a combination of hydrophobic forces and pi interactions, enhancing its potential as a therapeutic compound. The residues on daidzein compared to the residues on the ribavirin compound (control) are the residues on the hydrogen bond (Val411), the residues on the van der Waals bond (Phe412, and Trp795). This may indicate that myricetin and the control have similar binding mechanisms.

Fig. 3(f) shows that the interaction between the control ligand and the receptor forms a single bond, a hydrogen bond (green), with the control ligand forming hydrogen bonds with Asn405, Val411, Gly604, and Thr605. Van der Waals interactions with Lys401, Phe412, Ser600, Gly601, Gln602, Val603, Tyr606, Arg792, and Trp795. Ribavirin forms hydrogen bonds with Asn405, Val411, Gly604, and Thr605, which help stabilize the ligand-protein complex through specific bonds between the polar groups of ribavirin and the polar sides of residues at the active site. In addition, van der Waals interactions with Lys401, Phe412, Ser600, Gly601, Gln602, Val603, Tyr606, Arg792, and Trp795,

strengthen the hydrophobic bonds between ribavirin and the protein. Although these interactions indicate good bonding, ribavirin bonds are simpler compared to other compounds, such as flavonoids, which can involve stronger interactions, such as pi-stacking or electrostatic interactions.

Hydrogen bonds are one of the bonds that contribute to ΔG. Hydrogen bonds involve interactions between covalently bonded hydrogen atoms and electronegative atoms, such as nitrogen (N), fluorine (F), and oxygen (O) [43]. The hydrogen bonds formed originate from the native ligand's oxygen atoms covalently bonded to the hydrogen atoms of the amino acid residues. As a result of these hydrogen bonds, the native ligand can bind to the Gly604. The distance of the hydrogen bond at that residue is 1.88 Å. A hydrogen bond is considered strong if its bond length is greater than 1.85 Å. Therefore, in this study, it can be concluded that the hydrogen bond formed between the native ligand and Gly604 is strong. Arg792 and Trp795 play an essential role in the binding and stability of compounds at the target protein's active site. Trp795 interacts with quercetin, fisetin, and myricetin through pi-stacking, which strengthens the binding, while Arg792 interacts electrostatically with negative groups on the ligand, increasing the stability of the complex. Although daidzein interacts with both residues, the binding is weaker because it does not form strong hydrogen bonds [41].

The binding affinity, selected based on the most negative value, greatly affects the stability of the interactions between the ligands and the receptors. Negative values indicate lower energy required for the receptor to interact spontaneously with the ligand. The lower the binding affinity, the more stable the interaction between ligand and receptor. All compounds in the docking results showed different binding affinity values for each receptor, all with negative values. In DENV-3 RdRp (3VWS), quercetin had the lowest binding affinity value of −8.0 kcal/mol. An active compound is predicted to have the ability to interact with the target receptor if it has a binding affinity equal to or lower than that of the reference drug [7]. The results of binding affinity values are presented in Table 2.

The interactions between each ligand and amino acid residue involve several important residues in ligand-macromolecule interactions. In Fig. 3, we can see that residues Asn492, Gly601, Arg792, and Trp795 frequently appear in every ligand-receptor interaction in the form of hydrogen bonds and hydrophobic interactions, so these residues are predicted to play an important role in the binding site of the DENV-3 RdRp receptor. When bound to the DENV-3 RdRp receptor in the molecular docking, the quercetin showed a more negative binding affinity (−8.0 kcal/mol) compared to the reference ligand, ribavirin (−5.6 kcal/mol), and the native ligand (−7.7 kcal/mol). The lower binding affinity value indicates stronger bioactivity and a greater ability to interact with the target protein's binding site compared to the reference ligand [44]. Quercetin can potentially be used as an inhibitor of the DENV-3 RdRp receptor.

MD Simulation

MD simulations were carried out to overcome the limitations of the molecular docking process that treated the target protein as a rigid structure and overlooked the presence of water solvents in the interaction analysis [45]. In MD simulations, proteins were made flexible like ligands, and the role of water solvents was included. In some studies, the influence of water is significant in bridging the interaction between the protein and the ligand. The addition of water affects the energy of the simulated system [46]. The stability of the system can be observed using RMSD, root mean square fluctuation (RMSF), radius of gyration (RoG), and hydrogen bonds generated during the simulation.

Fig. 4 shows the RMSD value illustrating the positional changes of carbon atoms in the protein backbone during simulation. RMSD analysis in this study was performed to evaluate the ligand stability when interacting and forming complexes with proteins. This analysis measures the degree to which the ligand deviates from its initial conformation, a reference during simulation. Monitoring the RMSD over time makes it possible to assess the system's stability and identify periods of equilibrium and fluctuations. Higher RMSD values indicate greater structural deviations from the

Table 2. Molecular docking results and interactions of flavonoids with target ligands

Compound	Binding affinity	Hydrogen bond	Interaction type	Amino acid residue
Native ligand	−7.7	Gly604	Van der Waals	Asn405, Gln602, Gly601, Val603, Thr605, Tyr606, Trp795, Ser796, Arg792
			Carbon hydrogen bond	Val603
			Pi-alkyl	Arg481, Phe412, Trp477, Ile797
Quercetin	−8.0	Asn492, Ser798, Asn492, Gln602	van der Waals	Phe412, Trp795, Arg792, His801, Lys401, Gly604, Thr605, Gly601, Arg481
			Pi-alkyl	Val603, Ile797
Fisetin	−7.4	Asn492, Gly601, Trp795	van der Waals	Lys401, Phe412, Gly604, Arg481, Thr605, Tyr606, Ser796, Arg792
			Pi-alkyl	Val603, Ile797
Myricetin	−7.3	Gln602, Asn405	van der Waals	Tyr606, Val603, Gly604, Asn492, Val411, Arg792, Trp795, Gly601, Ser600, Thr605
Daidzein	−7.4	-	van der Waals	Phe398, Phe485, Lys401, Thr413
			Carbon hydrogen bond	Val411
			Pi-Pi stacked	Phe412, Trp795
			Pi-alkyl	Val603
			Pi-Pi shaped	Phe412, Trp795
Ligand control (Ribavirin)	−5.6	Val411, Asn405, Thr605, Gly604	van der Waals	Ser600, Gln602, Gly601, Trp795, Arg792, Lys401, Phe412, Val603, Tyr606

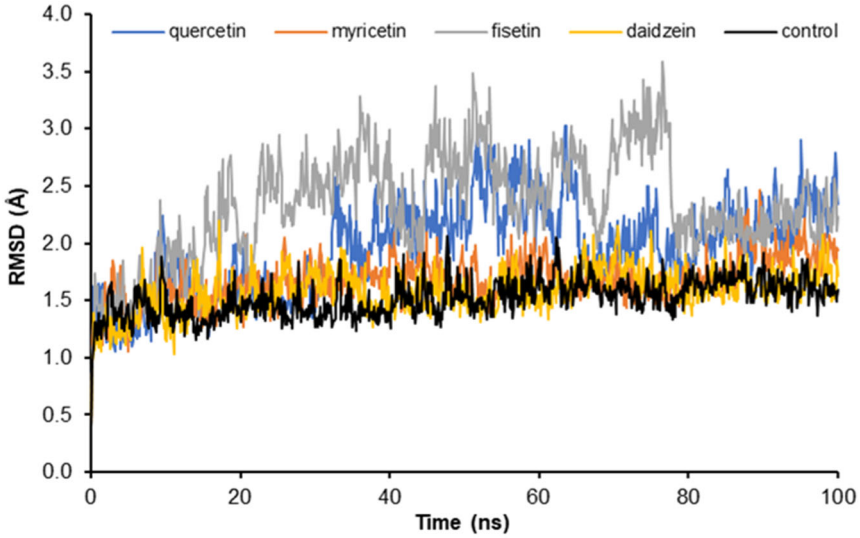

Fig 4. Comparison of RMSD values between compounds against DENV-3 RdRp

reference structure, suggesting increased flexibility or conformational changes. The greater the difference in ligand conformation and position during the simulation, the higher the RMSD value [47]. In drug discovery, ligands are expected to exhibit low RMSD values. RMSD values of 2–5 Å are generally considered acceptable for the system [48].

The average RMSD value of the ribavirin receptor (control) was 1.517 ± 0.16 Å. The RMSD graph in Fig. 4 shows that the ribavirin ligand maintained a stable value throughout the simulation. In contrast, the quercetin compound exhibited an increase in RMSD between 50 and 70 ns, reaching a peak value of 3.02 Å at 63.5 ns. The fisetin compound exhibited the highest increase in

RMSD between 0–100 ns, reaching a peak value of 3.587 Å at 76.6 ns. The myricetin compound showed an increase between 80 and 100 ns, with the highest RMSD value of 2.461 Å observed at 89.5 ns.

RMSD is an important metric in molecular dynamics simulations, particularly in the context of protein-ligand interactions and structural bioinformatics. It is an integral part of the scoring function in docking algorithms, which predict the binding pose of a ligand to a target protein [10]. RMSD analysis (Fig. 4) provides insights into the stability and conformational dynamics of DENV-3 RdRp when complexed with four flavonoid ligands (quercetin, fisetin, myricetin, and daidzein), compared to ribavirin as a control. During the 100 ns simulation period, an initial equilibration phase (0–20 ns) was observed, during which fluctuations gradually decreased as the complex stabilized. Beyond this phase, the RMSD values for each complex remained between 1.2 and 3.5 Å, indicating overall structural stability (Fig. 4).

Among the ligands tested, quercetin, fisetin, myricetin, and daidzein, compared with ribavirin as a control, showed consistently lower RMSD values during the simulation, indicating stable binding with minimal conformational changes. Specifically, the ribavirin complex (black line) achieved a stable RMSD range of approximately 1.2–2.0 Å after the equilibration phase, indicating highly stable interactions with the active polymerase site. The myricetin (orange) and daidzein (yellow) complexes followed the same trend, reflecting comparable binding stability. The quercetin (blue) and fisetin (gray) complexes, although relatively stable, exhibit slightly higher RMSD fluctuations than myricetin and daidzein, with values reaching approximately 2.5 Å, particularly in the second half of the simulation (around 70 ns). This behavior suggests that the quercetin ligand, although stable, allows for a modest degree of conformational flexibility in the polymerase compared to the myricetin, daidzein, and control ligand. Overall, the consistently lower and more stable RMSD values underscore their potential to provide more stable binding interactions with DENV-3 RdRp.

RMSF describes the conformational shifts of individual amino acid residues, providing insight into the flexibility of the protein or receptor. In this case, the receptor fluctuates and will change its conformation over time. The lower the RMSF values, the more stable the interaction between the ligand and amino acid, thereby contributing to a more stable DENV-3 RdRp complex compared to the test ligand. The RMSF value will broadly describe the conformational shift of each amino acid residue that gives protein flexibility [34]. The results of the RMSF graph are illustrated in Fig. 5.

By measuring fluctuations in the position of atoms in proteins, RMSF reveals how structural dynamics relate to biological function, aiding in the development of effective therapies. Lower RMSF values indicate more rigid and stable regions, while higher RMSF values indicate more flexible or dynamic regions in the protein structure. The fisetin (gray line) and myricetin complexes show very high RMSF values for some residues, particularly in the regions around 300–320 and 450–480, indicating local flexibility. Despite these fluctuations, the

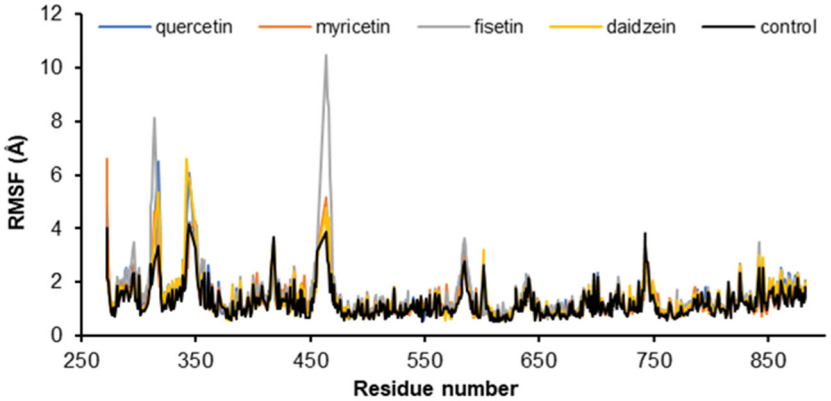

Fig 5. Comparison of RMSF values between compounds against DENV-3 RdRp

quercetin, daidzein, and control ligands maintain stable binding, suggesting that these ligands can induce flexibility in specific protein regions without compromising the overall stability of the complex. Other complexes, quercetin (blue), daidzein (yellow), and control (black) ligands, show relatively lower RMSF values throughout the protein, especially for ribavirin, indicating a relatively stable binding profile with minimal flexibility.

The lower RMSF values for quercetin indicate that quercetin does not induce significant conformational changes in the DENV-3 RdRp polymerase, consistent with its lowest binding free energy. The main fluctuations observed during the simulation occurred within specific amino acid residues, with RMSF values for ribavirin (control), quercetin, fisetin, myricetin, and daidzein recorded at 4.15 (residue 344), 6.52 (residue 317), 10.46 (residue 464), 6.59 (residue 272), and 6.60 (residue 342), respectively.

The RoG measures the distance between the center of mass of a protein's atoms and its terminal atoms within a specific period. The RoG of the flavonoid compounds against DENV-3 RdRp is shown in Fig. 6. Molecular dynamics simulation results showed that the average RoG values of the test compounds, ribavirin (control), quercetin, fisetin, myricetin, and daidzein were 25.99 ± 0.12; 26.32 ± 0.22; 26.36 ± 0.25; 25.98 ± 0.17; 25.97 ± 0.17 Å, respectively. The RoG analysis revealed no significant difference among the compounds, suggesting minimal structural change in ligand-receptor complexes.

Fig. 7 shows the number of hydrogen bonds formed during the simulation. Many estimated hydrogen bonds indicate a conformation similar to the simulation's initial structure. In contrast, a high RMSD value suggests that the ligand has moved away from the main catalytic amino acid residues, thereby reducing ligand–receptor hydrogen bond interactions.

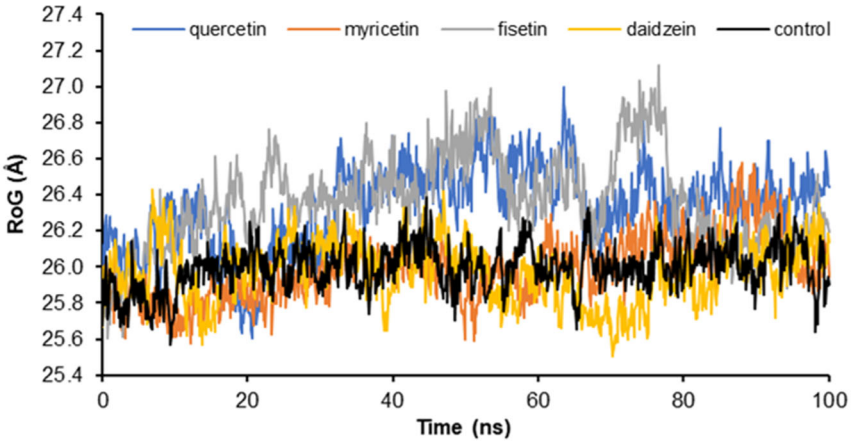

Fig 6. Comparison of RoG values between compounds against DENV-3 RdRp

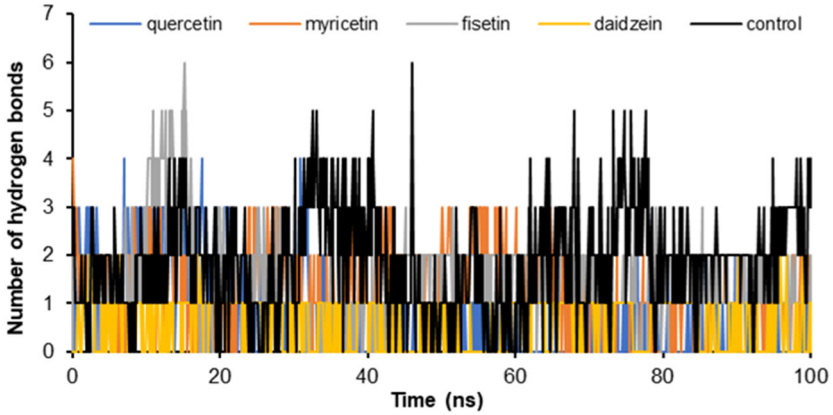

Fig 7. The number of hydrogen bonds between compounds and DENV-3 RdRp

Differences in protein-ligand hydrogen bond interactions were observed in the simulation. The highest number of hydrogen bonds was observed in ribavirin compounds (control), with six hydrogen bonds detected at 46.0 ns. In contrast, four hydrogen compounds were detected in the 30 ns in quercetin compounds. The fisetin compound also formed six hydrogen bonds, detected at 15.2 ns. Four hydrogen bonds were found in the myricetin compound at 0.1 ns, and the daidzein compound showed two hydrogen bonds at multiple time points:1.8, 2.5, 6.1, 6.3, 6.4, 10.8, and 11.3 ns.

The solvent accessible surface area (SASA) is related to protein compactness and is influenced by the simulation environment (Fig. 8). The more compact the protein, the lower the SASA value. The SASA calculates the surface area of the protein-ligand complex that can interact with solvent molecules. A decrease in SASA values in proteins indicates an increase in protein density and a decrease in exposure to the solvent [49]. In the DENV-3 RdRp complex (Fig. 8), the SASA value for quercetin averaged 26.022 Å, increased at 24 ns, then decreased and increased again at 42 ns, and began to stabilize at 80 ns. Fisetin, with an average SASA value of 26.712 Å, showed an increase in SASA at 65 ns, followed by a decrease at 72 ns, and stabilized at 85 ns. Myricetin and daidzein have almost the same average values, namely 26.021 and 26.091 Å, respectively, with a tolerable increase at 38 ns, but overall SASA values remained stable at 70 ns. These results indicate that all complexes are compact and stable at around 80 ns.

Bioactivity Analysis of Flavonoids

The PASS was used to predict the bioactivity spectra of flavonoids (quercetin, fisetin, myricetin, daidzein) Compound activity spectrum prediction (PASS) was used to predict the bioactivity spectrum of flavonoids (quercetin, fisetin, myricetin, daidzein) compared to antiviral compounds as positive controls (ribavirin) with mechanisms of action that inhibit virus entry and RNA synthesis [34]. PASS web server predicts various biological activities, but this study focuses on the prediction of antiviral agents and DENV-3 RdRp inhibitors. All flavonoid compounds (quercetin, fisetin, myricetin, daidzein) and the positive control ribavirin exhibited antiviral activity. They inhibited RNA synthesis and virus entry, except ribavirin, which does not show such activity. Previous studies have shown that fisetin, myricetin, and quercetin exhibit antiviral activity by inhibiting viral entry and RNA synthesis [13-14,44].

Table 3 shows that *in silico* prediction results using PASS indicate that ribavirin has a high potential as an antiviral agent (Pa = 0.806), making it a strong candidate for such activity. In contrast, other compounds such as quercetin, fisetin, myricetin, and daidzein exhibit lower potential for antiviral activity, with Pa values ranging from 0.182 to 0.334. However, most of these compounds exhibit moderate potential as RNA synthesis inhibitors, with Pa values between 0.320 and 0.371, suggesting that they may be effective in inhibiting RNA synthesis. Quercetin showed superior therapeutic potential compared to fisetin, myricetin, daidzein, and the control

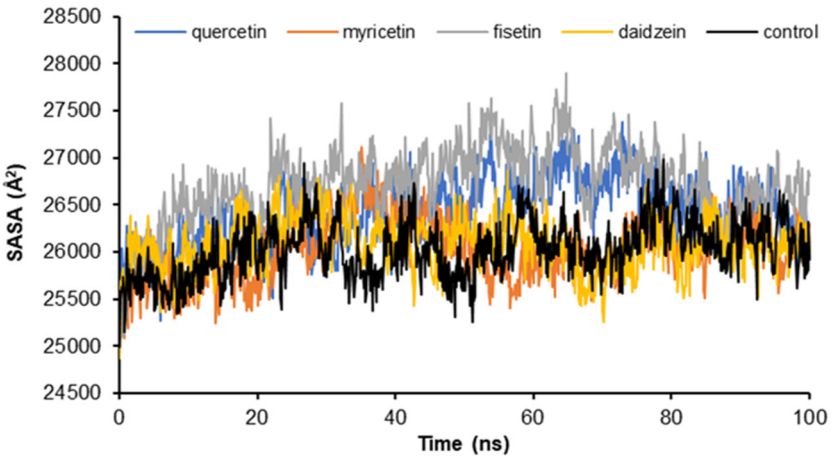

Fig 8. Comparison of the SASA values between several compounds against DENV-3 RdRp

Table 3. *In silico* PASS results

Compounds	Activities prediction	Pa	Pi
Quercetin	Antiviral	0.262	0.053
	Viral entry inhibitor	0.257	0.027
	RNA synthesis inhibitor	0.345	0.033
Fisetin	Antiviral	0.251	0.059
	Viral entry inhibitor	0.275	0.014
	RNA synthesis inhibitor	0.320	0.043
Myricetin	Antiviral	0.334	0.026
	Viral entry inhibitor	0.272	0.016
	RNA synthesis inhibitor	0.322	0.042
Daidzein	Antiviral	0.182	0.116
	Viral entry inhibitor	0.196	0.175
	RNA synthesis inhibitor	0.367	0.026
Ribavirin	Antiviral	0.806	0.004
	Viral entry inhibitor	-	-
	RNA synthesis inhibitor	0.371	0.025

compound (ribavirin). Although ribavirin has a higher Pa value for antiviral activity (0.806), quercetin exhibits a better balance between antiviral activity, viral entry inhibition, and RNA synthesis inhibition, with Pa values of 0.262, 0.257, and 0.345, respectively, and relatively low Pi values, indicating high efficacy with a low risk of failure. In addition, quercetin has stronger potential as an RNA synthesis inhibitor compared to other compounds such as fisetin and myricetin (with Pa values of 0.320 and 0.322, respectively). Ribavirin exhibits strong antiviral activity, with a lower Pa value for RNA synthesis inhibition (0.371) than quercetin, indicating that quercetin may be more effective in targeting several viral replication pathways, making it a more effective and potentially broader alternative compound in antiviral therapy for DENV.

Pharmacokinetic and ADME Predictions

Drug likeness refers to the suitability of a compound for oral administration of drugs related to its absorption and distribution. Good drug candidates must meet criteria, including adherence to established rules for developing and selecting drug candidates suitable for oral administration. A compound must meet five criteria known as "Lipinski's Rule of Five". These criteria include a molecular weight of < 500 g/mol, a log-P value (lipophilicity) of no higher than five, a maximum of five hydrogen bond donors, no more than 10 hydrogen bond acceptors, and a molar refractive index in the range of 40–130 [39].

The drug's molecular weight is related to the drug distribution process that penetrates the biological membrane through diffusion. Compounds with a molecular weight of > 500 g/mol may have difficulty penetrating the membrane, resulting in prolonged drug absorption time [39,50]. The lipophilicity value shows the nature of the solubility of a compound in fat and water. Meanwhile, the log P value indicates that the molecule has a high level of hydrophobicity. Hydrophobic molecules will have a greater level of toxicity because they remain bound to the lipid bilayer for more extended periods and are distributed more widely throughout the body. The number of hydrogen bonds between the donor and acceptor correlates with the biological activity of a compound. The higher the bonding capacity of the donor and acceptor, the greater the energy required for the absorption process to occur [33-34]. Bioavailability reflects the relationship between the dose of a drug and the amount that reaches the bloodstream. The human body can properly absorb a drug if its bioavailability value is equal to 0.55 [51]. Data on the application of Lipinski's rule can be seen in Table 4.

ADME analysis is essential for understanding how a drug reaches its target. The structures of the compounds obtained from the PubChem database were analyzed to determine whether they met the requirement criteria. Subsequently, the ADME profiles were calculated using the SwissADME server [52]. The analysis showed that most compounds met the ADME properties (Table 4).

This is illustrated in Fig. 9(a), which presents a radar plot depicting six ADME parameters related to the oral bioavailability of a compound, including LIPO (lipophility), SIZE (molecular size), POLAR (Polarity), INSOLU (Insolubility), INSATU (Instauration), and FLEX (Flexibility). Based on the bioavailability radar, flavonoid compounds (quercetin, fisetin, myricetin, and daidzein) demonstrate strong potential as drug candidates. Five ADME parameters fall within the optimal pink zone, with only one parameter in the white

Table 4. Drug scan test results according to Lipinski's Rule of Five

Compound	Parameters					
	Formula	Molecular weight < 500 (g/mol)	H-bond acceptor < 10	H-bond donors < 5	log P <5	Bioavailability
Quercetin	$C_{15}H_{10}O_7$	302.24	7	5	1.63	0.55
Fisetin	$C_{15}H_{10}O_6$	286.24	6	4	1.50	0.55
Myricetin	$C_{15}H_{10}O_8$	318.24	8	6	1.08	0.55
Daidzein	$C_{15}H_{10}O_4$	254.24	4	2	1.77	0.55
Ribavirin	$C_8H_{12}N_4O_5$	244.20	7	4	0.35	0.55

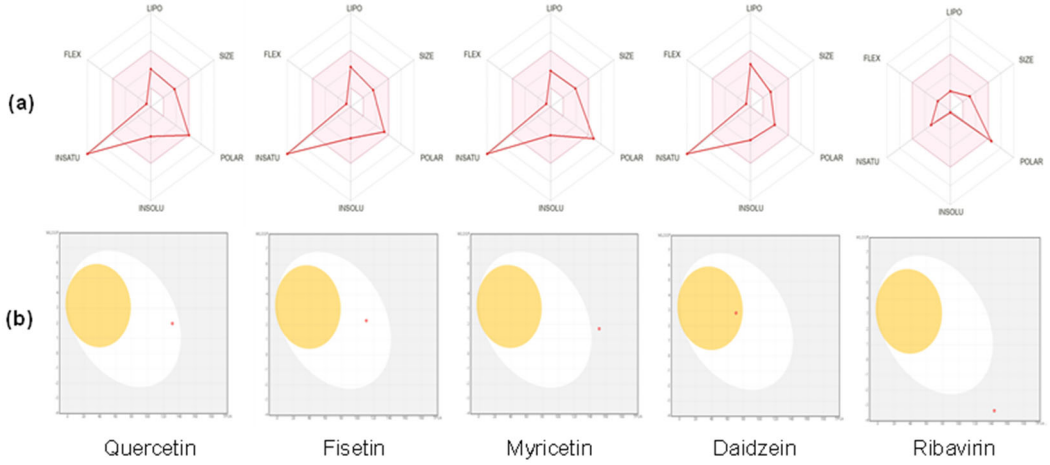

Fig 9. SwissADME (a) bioavailability radar and (b) boiled-egg models

area, indicating favorable oral bioavailability profiles. A molecule whose radar plot entirely resides within the pink area suggests good potential as a drug candidate, as this region represents the optimal range for each ADME parameter [53].

The results of ADME predictions indicate that quercetin, fisetin, and daidzein have high gastrointestinal absorption (HIA) capabilities, facilitating absorption in the digestive tract. In contrast, myricetin and daidzein have low gastrointestinal absorption capabilities due to their low water solubility and relatively high polarity, making them difficult to dissolve and absorb in the intestines. Additionally, flavonoids like myricetin often undergo pre-systemic metabolism (e.g., by enzymes in the intestines and liver), reducing the amount of active compounds that reach the circulation. Daidzein also has low bioavailability due to its natural glycosidic bonds, which must first be hydrolyzed by gut microbiota before absorption [54].

Fig. 9(b) shows that all compounds exhibit high HIA, facilitating efficient absorption in the gastrointestinal tract. However, myricetin and ribavirin exhibit limited gastrointestinal absorption due to several factors, including first-pass metabolism, low lipophilicity, and limited transporters, all hindering their bioavailability. These factors contribute to ribavirin's relatively low oral bioavailability, despite its effectiveness in viral infection treatment [55]. According to ADME predictions, no compounds penetrate the blood-brain barrier except daidzein. One of the significant factors influencing a compound's ability to penetrate the blood-brain barrier (BBB) is its lipophilicity. Daidzein is a lipophilic (fat-soluble) compound, which allows this molecule to pass through the lipid-rich cell membranes that form the BBB. All compounds showed to be non-inhibitors of P-gp substrates, suggesting they do not interfere with the distribution process or bioavailability of the drug [54].

The Boiled-Egg Analysis in pharmacokinetic profile prediction assesses a compound's ability to penetrate and undergo passive absorption in the gastrointestinal region. This analysis considers two physicochemical properties: TPSA and WLOGP, to evaluate lipophilicity and polarity. The red circle in the Boiled-Egg diagram (Fig. 9(b)) indicates that the compound does not pass through P-glycoprotein, meaning the compound remains within the target cells. The red point in the yellow area indicates that the compound can passively penetrate the BBB [53]. Fig. 9(b) indicates that four compounds (quercetin, fisetin, myricetin, and ribavirin) cannot penetrate the blood-brain barrier, while one compound, daidzein, can passively penetrate the BBB.

Based on Table 5, the drug metabolism process is carried out by enzymes in the endoplasmic reticulum membrane of liver cells. Drugs can undergo two types of metabolism to convert them into more polar compounds, one of which is phase I reactions involving oxidation, reduction, or hydrolysis reactions. These reactions involve enzymes containing cytochrome P450 with isoenzymes that play an important role in the metabolism of endogenous compounds capable of catalyzing oxidative biological changes, namely CYP. Important isoenzymes include CYP1A2, CYP2C9, CYP2D6, CYP2E1, CYPC19 and CYP3A4 [56]. Quercetin showed metabolic activity as inhibitors of CYP1A2, CYP2C8, CYP2D6 [57], CYP2B [58], and CYP3A4 [59]. Fisetin, myricetin, and daidzein also inhibit CYP3A4 enzymes [59], unlike the positive control ribavirin. However, none of these five compounds inhibited the CYP2C9 and CYP2C19 isoenzymes. Interpretation of the interaction between compounds and CYP3A4 enzymes in compound metabolism analysis. CYP3A4 enzymes are one of the isoforms of cytochrome P450 enzymes that play an important role in drug metabolism in the liver. These enzymes are involved in the oxidation of lipophilic compounds, which often change the structure of drugs into forms that are more easily eliminated through urine or bile. The interaction of compounds with CYP3A4 is very important to consider because it can affect the metabolic rate and bioavailability of compounds in the body. In this study, the prediction results indicate that some of the flavonoids we evaluated have the potential to interact with CYP3A4, which can modulate the metabolism of these compounds. For example, quercetin, one of the flavonoids tested, has been reported to inhibit CYP3A4 activity [60].

Based on this research, four flavonoid compounds (quercetin, fisetin, myricetin, daidzein), compared to antiviral compounds as positive controls (ribavirin), have mechanisms of action that inhibit virus entry and RNA synthesis according to three criteria: Lipinski, Ghose, and Veber. The results show that quercetin and fisetin meet all three criteria, indicating that both have properties that support them as drug candidates. Myricetin meets the Lipinski and Ghose criteria but does not meet the Veber criterion, suggesting that while it has good properties, myricetin may have limitations in molecular flexibility. Daidzein meets all criteria except Veber, meaning that while it has nearly ideal properties, daidzein is less optimal in terms of molecular flexibility. Meanwhile, ribavirin, which was used as a control, only met Lipinski's criteria and did not meet the criteria set by Ghose and Veber.

Analysis of drug-likeness can be assessed using Lipinski's, Ghose's, and Veber's rules. Lipinski's rules show the physicochemical and hydrophobic/hydrophilic properties of compounds that can pass through cell

Table 5. The pharmacokinetic properties of flavonoid compounds

Compound	Pharmacokinetic properties								
	GI absorption	P-gp substrate	BBB permeant	CYPIA2	CYP2D6	CYP2C9	CYP2C19	CYP3A4	Bioavailability
Quercetin	High	No	No	Yes	Yes	No	No	Yes	0.55
Fisetin	High	No	No	Yes	Yes	No	No	Yes	0.55
Myricetin	Low	No	No	Yes	No	No	No	Yes	0.55
Daidzein	High	No	Yes	Yes	Yes	No	No	Yes	0.55
Ribavirin (control)	Low	No	No	No	No	No	No	No	0.55

Table 6. Drug-likeness properties of flavonoid compounds

Compound	Lipinski	Ghose	Veber
Quercetin	Yes	Yes	Yes
Fisetin	Yes	Yes	Yes
Myricetin	Yes	Yes	No
Daidzein	Yes	Yes	Yes
Ribavirin (control)	Yes	No	No

membranes by passive diffusion. In contrast, Ghose's rules use parameters such as molecular weight, log P (lipophilicity), and polarity index to assess the potential of compounds as drugs that can penetrate biological membranes (such as cell membranes or blood-brain barrier). Potential drug candidates with favorable bioavailability can be efficiently absorbed into the body. The drug-likeness properties in Table 6 show that all flavonoids and the positive control ribavirin meet Lipinski's rules. However, ribavirin, as a positive control, did not meet the criteria established by Ghose and Vabe, having a low log P (0.35) and thus being very hydrophilic and poor in penetrating cell membranes, even though it is effective in treating viral infections by other mechanisms [61-62].

■ CONCLUSION

In this study, we performed an *in silico* analysis of quercetin, fisetin, myricetin, daidzein, and one control compound, ribavirin. The order of bond energies from the weakest to the strongest as follows: quercetin, daidzein, fisetin, myricetin, and ribavirin. Quercetin is the most promising candidate among these compounds because it has the lowest binding energy (−8.0 kcal/mol). MD simulations for 100 ns showed that the DENV-3 RdRp complex structure was stable. The initial and final conformations of the DENV-3 RdRp complex from MD simulations indicate that the test ligands interact well with the main amino acid residues. Thus, the clearly observed non-covalent interactions suggest that these flavonoids have antiviral activity against DENV based on the inhibition of RdRp replication. Swiss-ADME predictions indicate that all five compounds meet Lipinski's rules, suggesting potential oral bioavailability and good drug-like properties. Based on molecular docking mapping, MD simulations, ADME analysis, and bioactivity testing results, quercetin shows promising potential as an inhibitor of DENV. The strong interaction between quercetin and the active site of the viral protein, the stability demonstrated in MD simulations, and its favorable pharmacokinetic profile make it a viable candidate for further development. *In vitro* testing will further prove quercetin's inhibitory activity against Dengue virus replication under more biologically relevant conditions.

■ ACKNOWLEDGMENTS

The authors would like to thank *Direktorat Riset, Teknologi, dan Pengabdian kepada Masyarakat* (DRTPM) No. 0536/E5/PG.02.00/2023 for providing this research funding. The authors would also like to thank Prof. Dr.rer.nat. Harno Dwi Pranowo, M.S., and the Austrian-Indonesian Center (AIC) Laboratory for Computational Chemistry at the Department of Chemistry, Faculty of Mathematics and Natural Sciences, Universitas Gadjah Mada, for available computing facilities.

■ CONFLICT OF INTEREST

All the authors have no conflict of interest.

■ AUTHOR CONTRIBUTIONS

Siti Zainatun Wasilah: Conceptualization, Original Draft Preparation, Data Curation, Writing – Review & Editing, Validation. Tri Wibawa: Supervision, Data Curation, Writing – Review & Editing, Validation, Investigation. Nastiti Wijayanti: Visualization, Investigation, Validation, Supervision, Writing – Review & Editing. All authors have read and agreed to the final version of the manuscript.

■ REFERENCES

[1] Hershan, A.A., 2023, Dengue virus: Molecular biology and recent developments in control strategies, prevention, management, and therapeutics, *J. Pharmacol. Pharmacother.*, 14 (2), 107–124.

[2] Khan, M.B., Yang, Z.S., Lin, C.Y., Hsu, M.C., Urbina, A.N., Assavalapsakul, W., Wang, W.H., Chen, Y.H., and Wang, S.F., 2023, Dengue overview: An updated systemic review, *J. Infect. Public Health*, 16 (10), 1625–1642.

[3] Mustafa, M.S., Rasotgi, V., Jain, S., and Gupta, V., 2015, Discovery of fifth serotype of dengue virus (DENV-5): A new public health dilemma in dengue control, *Med. J. Armed Forces India*, 71 (1), 67–70.

[4] Hossain, M.I., Alam, N.E., Akter, S., Suriea, U., Aktar, S., Shifat, S.K., Islam, M.M., Aziz, I., Islam, M.M., Islam, M.S., and Mohiuddin, A.K.M., 2021, Knowledge, awareness and preventive practices of dengue outbreak in Bangladesh: A countrywide study, *PLoS One*, 16 (6), e0252852.

[5] Thomas, S.J., 2023, Is new dengue vaccine efficacy data a relief or cause for concern?, *npj Vaccines*, 8 (1), 55.

[6] Lee, M.F., Wu, Y.S., and Poh, C.L., 2023, Molecular mechanisms of antiviral agents against dengue virus, *Viruses*, 15 (3), 705.

[7] Monsalve-Escudero, L.M., Loaiza-Cano, V., Zapata-Cardona, M.I., Quintero-Gil, D.C., Hernández-Mira, E., Pájaro-González, Y., Oliveros-Díaz, A.F., Diaz-Castillo, F., Quiñones, W., Robledo, S., and Martinez-Gutierrez, M., 2021, The antiviral and virucidal activities of voacangine and structural analogs extracted from *Tabernaemontana cymosa* depend on the dengue virus strain, *Plants*, 10 (7), 1280.

[8] Kausar, M.A., Ali, A., Qiblawi, S., Shahid, S.M.A., Izhari, M.A., and Saral, A., 2019, Molecular docking based design of dengue NS5 methyltransferase inhibitors, *Bioinformation*, 15 (6), 394–401.

[9] Shimizu, H., Saito, A., Mikuni, J., Nakayama, E.E., Koyama, H., Honma, T., Shirouzu, M., Sekine, S., and Shioda, T., 2019, Discovery of a small molecule inhibitor targeting dengue virus NS5 RNA-dependent RNA polymerase, *PLoS Neglected Trop. Dis.*, 13 (11), e0007894.

[10] Hasan, M.Z., Soikot, S., Hossain, M.M., Priota, M.F., Akther, S., Jahan, S., Bhuyian, J., Sharul, N.R., Hossain, M.M., Al Jubayed, M.A., Rahman, N., Mawya, J., Akter, N., Hosen, M.E., and Faruqe, M.O., 2025, Discovering potential inhibitors against dengue virus NS5 RNA dependent RNA polymerase from local vegetables: A comparative computational study, *Discover Chem.*, 2 (1), 120.

[11] Pandey, P., Rane, J.S., Chatterjee, A., Kumar, A., Khan, R., Prakash, A., and Ray, S., 2021, Targeting SARS-CoV-2 spike protein of COVID-19 with naturally occurring phytochemicals: An *in silico* study for drug development, *J. Biomol. Struct. Dyn.*, 39 (16), 6306–6316.

[12] Joshi, R.S., Jagdale, S.S., Bansode, S.B., Shankar, S.S., Tellis, M.B., Pandya, V.K., Chugh, A., Giri, A.P., and Kulkarni, M.J., 2021, Discovery of potential multi-target-directed ligands by targeting host-specific SARS-CoV-2 structurally conserved main protease, *J. Biomol. Struct. Dyn.*, 39 (9), 3099–3114.

[13] Badshah, S.L., Faisal, S., Muhammad, A., Poulson, B.G., Emwas, A.H., and Jaremko, M., 2021, Antiviral activities of flavonoids, *Biomed. Pharmacother.*, 140, 111596.

[14] Terefe, E.M., Okalebo, F.A., Derese, S., Muriuki, J., and Batiha, G.E.S., 2021, *In vitro* cytotoxicity and anti-HIV activity of crude extracts of *Croton macrostachyus*, *Croton megalocarpus* and *Croton dichogamus*, *J. Exp. Pharmacol.*, 13, 971–979.

[15] LaManna, J.C., Puchowicz, M.A., Xu, K., Harrison, D.K., and Bruley, D.F., 2011, Oxygen transport to tissue XXXII, *Adv. Exp. Med. Biol.*, 701, XXX, 374.

[16] Jadaun, A., Subbarao, N., and Dixit, A., 2017, Allosteric inhibition of topoisomerase I by pinostrobin: Molecular docking, spectroscopic and topoisomerase I activity studies, *J. Photochem. Photobiol., B*, 167, 299–308.

[17] Hsu, M.C., Dhingra, U., Earley, J.V., Holly, M., Keith, D., Nalin, C.M., Richou, A.R., Schutt, A.D., Tam, S.Y., and Potash, M.J., 1993, Inhibition of type 1 human immunodeficiency virus replication by a Tat antagonist to which the virus remains sensitive after prolonged exposure *in vitro*, *Proc. Natl. Acad. Sci. U. S. A.*, 90 (14), 6395–6399.

[18] Palanichamy Kala, M., St. John, A.L., and Rathore, A.P.S., 2023, Dengue: Update on clinically relevant therapeutic strategies and vaccines, *Curr. Treat. Options Infect. Dis.*, 15 (2), 27–52.

[19] Rojas, N., Del Campo, J.A., Clement, S., Lemasson, M., García-Valdecasas, M., Gil-Gómez, A., Ranchal, I., Bartosch, B., Bautista, J.D., Rosenberg,

A.R., Negro, F., and Romero-Gómez, M., 2016, Effect of quercetin on hepatitis C virus life cycle: From viral to host targets, *Sci. Rep.*, 6 (1), 31777.

[20] Wu, W., Li, R., Li, X., He, J., Jiang, S., Liu, S., and Yang, J., 2016, Quercetin as an antiviral agent inhibits influenza A virus (IAV) entry, *Viruses*, 8 (1), 6.

[21] Zandi, K., Teoh, B.T., Sam, S.S., Wong, P.F., Mustafa, M.R., and Abubakar, S., 2011, Antiviral activity of four types of bioflavonoid against dengue virus type-2, *Virol. J.*, 8 (1), 560.

[22] Sun, Y., Li, C., Li, Z., Shangguan, A., Jiang, J., Zeng, W., Zhang, S., and He, Q., 2021, Quercetin as an antiviral agent inhibits the Pseudorabies virus *in vitro* and *in vivo*, *Virus Res.*, 305, 198556.

[23] Lani, R., Hassandarvish, P., and AbuBakar, S., 2025, Fisetin limits chikungunya virus-induced apoptosis hallmarks in hepatocellular carcinoma cells, *Sci. Rep.*, 15 (1), 25140.

[24] Kang, S.Y., Kang, J.Y., and Oh, M.J., 2012, Antiviral activities of flavonoids isolated from the bark of *Rhus verniciflua* stokes against fish pathogenic viruses *in vitro*, *J. Microbiol.*, 50 (2), 293–300.

[25] Muñoz, A.L., Cuéllar, A.F., Arévalo, G., Santamaría, B.D., Rodríguez, A.K., Buendía-Atencio, C., Reyes Chaparro, A., Tenorio Barajas, A.Y., Segura, N.A., Bello, F., Suárez, A.I., Rangel, H.R., and Losada-Barragán, M., 2023, Antiviral activity of myricetin glycosylated compounds isolated from *Marcetia taxifolia* against chikungunya virus, *EXCLI J.*, 22, 716–731.

[26] Li, W., Xu, C., Hao, C., Zhang, Y., Wang, Z., Wang, S., and Wang, W., 2020, Inhibition of herpes simplex virus by myricetin through targeting viral gD protein and cellular EGFR/PI3K/Akt pathway, *Antiviral Res.*, 177, 104714.

[27] Horio, Y., Sogabe, R., Shichiri, M., Ishida, N., Morimoto, R., Ohshima, A., and Isegawa, Y., 2020, Induction of a 5-lipoxygenase product by daidzein is involved in the regulation of influenza virus replication, *J. Clin. Biochem. Nutr.*, 66 (1), 36–42.

[28] Tatura, S.N.N., Denis, D., Santoso, M.S., Hayati, R.F., Kepel, B.J., Yohan, B., and Sasmono, R.T., 2021, Outbreak of severe dengue associated with DENV-3 in the city of Manado, North Sulawesi, Indonesia, *Int. J. Infect. Dis.*, 106, 185–196.

[29] Hakim, F.K.N., Aryati, A., Sunari, I.G.A.A.E.P., Tanzilia, M., and Indrasari, Y.N., 2024, Viral load and the effect to severity of dengue: Does it really matter?, *J. Med. Chem. Sci.*, 7 (10), 1277–1286.

[30] Hasan, M.M., Khan, Z., Chowdhury, M.S., Khan, M.A., Moni, M.A., and Rahman, M.H., 2022, *In silico* molecular docking and ADME/T analysis of quercetin compound with its evaluation of broad-spectrum therapeutic potential against particular diseases, *Inf. Med. Unlocked*, 29, 100894.

[31] Trott, O., and Olson, A.J., 2010, AutoDock Vina: Improving the speed and accuracy of docking with a new scoring function, efficient optimization, and multithreading, *J. Comput. Chem.*, 31 (2), 455–461.

[32] Krieger, E., and Vriend, G., 2014, YASARA View-molecular graphics for all devices-from smartphones to workstations, *Bioinformatics*, 30 (20), 2981–2982.

[33] Istyastono, E.P., and Prasasty, V.D., 2021, Computer-aided discovery of pentapeptide AEYTR as a potent acetylcholinesterase inhibitor, *Indones. J. Chem.*, 21 (1), 243–250.

[34] Fatriansyah, J.F., Rizqillah, R.K., and Yandi, M.Y., 2022, Molecular docking and molecular dynamics simulation of fisetin, galangin, hesperetin, hesperidin, myricetin, and naringenin against polymerase of dengue virus, *J. Trop. Med.*, 2022 (1), 7254990.

[35] Mena-Ulecia, K., Tiznado, W., and Caballero, J., 2015, Study of the differential activity of thrombin inhibitors using docking, QSAR, molecular dynamics, and MM-GBSA, *PLoS One*, 10 (11), e0142774.

[36] Kumar, S., Bajrai, L.H., Faizo, A.A., Khateb, A.M., Alkhaldy, A.A., Rana, R., Azhar, E.I., and Dwivedi, V.D., 2022, Pharmacophore-model-based drug repurposing for the identification of the potential inhibitors targeting the allosteric site in dengue virus NS5 RNA-dependent RNA polymerase, *Viruses*, 14 (8), 1827.

[37] Bhattarai, B.R., Adhikari, B., Basnet, S., Shrestha, A., Marahatha, R., Aryal, B., Rayamajhee, B., Poudel, P., and Parajuli, N., 2022, *In silico* elucidation of potent

inhibitors from natural products for nonstructural proteins of dengue virus, *J. Chem.*, 2022 (1), 5398239.

[38] Du, B.X., Xu, Y., Yiu, S.M., Yu, H., and Shi, J.Y., 2023, ADMET property prediction via multi-task graph learning under adaptive auxiliary task selection, *iScience*, 26 (11), 108285.

[39] Rahman, T., Bappi, M.S.H., and Hossain, T.J., 2024, Prodigiosin demonstrates promising antiviral activity against dengue virus and zika virus in *in-silico* study, *Anal. Sci. Adv.*, 5 (11-12), e202400039.

[40] Filimonov, D.A., Lagunin, A.A., Gloriozova, T.A., Rudik, A.V., Druzhilovskii, D.S., Pogodin, P.V., and Poroikov, V.V., 2014, Prediction of the biological activity spectra of organic compounds using the PASS online web resource, *Chem. Heterocycl. Compd.*, 50 (3), 444–457.

[41] Anusuya, S., and Gromiha, M.M., 2017, Quercetin derivatives as non-nucleoside inhibitors for dengue polymerase: Molecular docking, molecular dynamics simulation, and binding free energy calculation, *J. Biomol. Struct. Dyn.*, 35 (13), 2895–2909.

[42] Ambarsari, L., Nur, N.A., Zanah, S.S.R., Kurniawanti, K., Dianhar, H., Warnasih, S., Cahyaning Rahayu, D.U., and Sugita, P., 2024, Molecular docking of biflavonoids from genus araucaria as DENV NS5 RNA-dependent RNA polymerase inhibitor using YASARA and Plants programs, *Int. J. Appl. Pharm.*, 16 (5), 291–299.

[43] Derewenda, Z.S., 2023, C-H groups as donors in hydrogen bonds: A historical overview and occurrence in proteins and nucleic acids, *Int. J. Mol. Sci.*, 24 (17), 13165.

[44] Fakih, T.M., Ramadhan, D.S.F., and Darusman, F., 2021, Biological activity, molecular docking, and ADME predictions of amphibine analogues of *Ziziphus spina-christi* towards SARS-CoV-2 M^{pro}, *Biogenesis*, 9 (1), 109–117.

[45] Chen, Y.C., 2015, Beware of docking!, *Trends Pharmacol. Sci.*, 36 (2), 78–95.

[46] Liu, L., Shao, S., Tu, Q., Gong, C., and Tian, B., 2024, Molecular dynamics simulation on the variations in characteristics of aqueous solution with diverse additives: Inspirations for binary ice preparation, *J. Mol. Liq.*, 411, 125820.

[47] Schreiner, W., Karch, R., Knapp, B., and Ilieva, N., 2012, Relaxation estimation of RMSD in molecular dynamics immunosimulations, *Comput. Math. Methods Med.*, 2012 (1), 173521.

[48] Pang, M., He, W., Lu, X., She, Y., Xie, L., Kong, R., and Chang, S., 2023, CoDock-Ligand: Combined template-based docking and CNN-based scoring in ligand binding prediction, *BMC Bioinf.*, 24 (1), 444.

[49] Islam, M.T., Aktaruzzaman, M., Barai, C., Rafi, F.I., Hasan, A.R., Tasnim, T., Sarder, P., Albadrani, G.M., Al-Ghadi, M.Q., Sayed, A.A., Abdel-Daim, M.M., Dona, H.A., Sarkar, K.K., and Raihan, M.O., 2025, *In silico* screening of naturally derived dietary compounds as potential butyrylcholinesterase inhibitors for Alzheimer's disease treatment, *Sci. Rep.*, 15 (1), 17134.

[50] Ali, M., Hassan, M., Ansari, S.A., Alkahtani, H.M., Al-Rasheed, L.S., and Ansari, S.A., 2024, Quercetin and kaempferol as multi-targeting antidiabetic agents against mouse model of chemically induced type 2 diabetes, *Pharmaceuticals*, 17 (6), 757.

[51] Murthy, T.P.K., Joshi, T., Gunnan, S., Kulkarni, N., Priyanka, V., Kumar, S.B., and Gowrishankar, B.S., 2021, *In silico* analysis of *Phyllanthus amarus* phytochemicals as potent drugs against SARS-CoV-2 main protease, *Curr. Res. Green Sustainable Chem.*, 4, 100159.

[52] Ghannay, S., Aouadi, K., Kadri, A., and Snoussi, M., 2022, *In vitro* and *in silico* screening of anti-*Vibrio* spp., antibiofilm, antioxidant and anti-quorum sensing activities of *Cuminum cyminum* L. volatile oil, *Plants*, 11 (17), 2236.

[53] Daina, A., Michielin, O., and Zoete, V., 2017, SwissADME: A free web tool to evaluate pharmacokinetics, drug-likeness and medicinal chemistry friendliness of small molecules, *Sci. Rep.*, 7 (1), 42717.

[54] Harahap, I.A., Olejnik, A., Kowalska, K., and Sulibursk a, J., 2024, Effects of daidzein, tempeh, and a probiotic digested in an artificial gastrointestinal

tract on calcium deposition in human osteoblast-like saos-2 cells, *Int. J. Mol. Sci.*, 25 (2), 1008.

[55] Preston, S.L., Drusano, G.L., Glue, P., Nash, J., Gupta, S.K., and McNamara, P., 1999, Pharmacokinetics and absolute bioavailability of ribavirin in healthy volunteers as determined by stable-isotope methodology, *Antimicrob. Agents Chemother.*, 43 (10), 2451–2456.

[56] Zhao, M., Ma, J., Li, M., Zhang, Y., Jiang, B., Zhao, X., Huai, C., Shen, L., Zhang, N., He, L., and Qin, S., 2021, Cytochrome P450 enzymes and drug metabolism in humans, *Int. J. Mol. Sci.*, 22 (23), 12808.

[57] Bojić, M., Kondža, M., Rimac, H., Benković, G., and Maleš, Ž., 2019, The effect of flavonoid aglycones on the CYP1A2, CYP2A6, CYP2C8 and CYP2D6 enzymes activity, *Molecules*, 24 (17), 3174.

[58] Kondža, M., Mandić, M., Ivančić, I., Vladimir-Knežević, S., and Brizić, I., 2023, *Artemisia annua* L. extracts irreversibly inhibit the activity of CYP2B6 and CYP3A4 enzymes, *Biomedicines*, 11 (1), 232.

[59] Kondža, M., Brizić, I., and Jokić, S., 2024, Flavonoids as CYP3A4 inhibitors *in vitro*, *Biomedicines*, 12 (3), 644.

[60] Zheng, W., Wu, H., Wang, T., Zhan, S., and Liu, X., 2021, Quercetin for COVID-19 and DENGUE co-infection: A potential therapeutic strategy of targeting critical host signal pathways triggered by SARS-CoV-2 and DENV, *Briefings Bioinf.*, 22 (6), bbab199.

[61] Te, H.S., Randall, G., and Jensen, D.M., 2007, Mechanism of action of ribavirin in the treatment of chronic hepatitis C, *Gastroenterol. Hepatol.*, 3 (3), 218–225.

[62] Helenius, A., 2018, Virus entry: Looking back and moving forward, *J. Mol. Biol.*, 430 (13), 1853–1862.